IEEE Access
Multidisciplinary : Rapid Review : Open Access Journal

Received 1 November 2023, accepted 14 November 2023, date of publication 16 November 2023, date of current version 22 November 2023.

Digital Object Identifier 10.1109/ACCESS.2023.3333752

RESEARCH ARTICLE

Endoscopic Image Analysis for Gastrointestinal Tract Disease Diagnosis Using Nature Inspired Algorithm With Deep Learning Approach

ABDULRAHMAN ALRUBAN[1], EATEDAL ALABDULKREEM[2], MAJDY M. ELTAHIR[3], ABDULLAH ALHARBI[4], IMÈNE ISSAOUI[5], AND AHMED SAYED[6]

[1]Department of Information Technology, College of Computer and Information Sciences, Majmaah University, Al Majma'ah 11952, Saudi Arabia
[2]Department of Computer Sciences, College of Computer and Information Sciences, Princess Nourah bint Abdulrahman University, Riyadh 11671, Saudi Arabia
[3]Department of Information Systems, College of Science and Art at Mahayil, King Khalid University, Abha 62529, Saudi Arabia
[4]Department of Computer Science, Community College, King Saud University, Riyadh 11437, Saudi Arabia
[5]Unit of Scientific Research, Applied College, Qassim University, Buraydah 52571, Saudi Arabia
[6]Research Center, Future University in Egypt, New Cairo 11835, Egypt

Corresponding author: Abdulrahman Alruban (a.alruban@mu.edu.sa)

The authors extend their appreciation to the Deanship of Scientific Research at King Khalid University for funding this work through large group Research Project under grant number (RGP2/29/44). Princess Nourah bint Abdulrahman University Researchers Supporting Project number (PNURSP2023R161), Princess Nourah bint Abdulrahman University, Riyadh, Saudi Arabia. Research Supporting Project number (RSP2022R444), King Saud University, Riyadh, Saudi Arabia. This study is partially funded by the Future University in Egypt (FUE).

ABSTRACT Endoscopic image analysis has played a pivotal function in the diagnosis and management of gastrointestinal (GI) tract diseases. Gastrointestinal endoscopy is a medical procedure where a flexible tube with an endoscope (camera) is inserted into the GI tract to visualize the inner lining of the colon, esophagus, stomach, and small intestine. The videos and images attained during endoscopy provide valuable data for detecting and monitoring a large number of GI diseases. Computer-assisted automated diagnosis technique helps to achieve accurate diagnoses and provide the patient the relevant medical care. Machine learning (ML) and deep learning (DL) methods have been exploited to endoscopic images for classifying diseases and providing diagnostic support. Convolutional Neural Networks (CNN) and other DL algorithms can learn to discriminate between various kinds of GI lesions based on visual properties. This study presents an Endoscopic Image Analysis for Gastrointestinal Tract Disease Diagnosis using an inspired Algorithm with Deep Learning (EIAGTD-NIADL) technique. The EIAGTD-NIADL technique intends to examine the endoscopic images using nature nature-inspired algorithm with a DL model for gastrointestinal tract disease detection and classification. To pre-process the input endoscopic images, the EIAGTD-NIADL technique uses a bilateral filtering (BF) approach. For feature extraction, the EIAGTD-NIADL technique applies an improved ShuffleNet model. To improve the efficacy of the improved ShuffleNet model, the EIAGTD-NIADL technique uses an improved spotted hyena optimizer (ISHO) algorithm. Finally, the classification process is performed by the use of the stacked long short-term memory (SLSTM) method. The experimental outcomes of the EIAGTD-NIADL system can be confirmed on benchmark medical image datasets. The obtained outcomes demonstrate the promising results of the EIAGTD-NIADL approach over other models.

INDEX TERMS Image processing, nature-inspired algorithms, deep learning, endoscopy images, gastrointestinal tract diseases.

I. INTRODUCTION

Gastrointestinal (GI) diseases are widespread in the human digestive system. A major popular corresponding to fatalities and occurrences namely Esophageal cancer, colorectal cancer, and stomach cancer are [1]. Endoscopic analyses are required for diagnosing diseases and usually make the serious earlier action to detect GI tract diseases. These analyses also increase the diagnostic of medical features of diseases for identifying their category and seriousness and to reach suitable analyses [2]. Differences in the capability of various physicians have introduced errors in any condition,

The associate editor coordinating the review of this manuscript and approving it for publication was Carmelo Militello.

particularly in terms of disputed issues of analytic videos and images from endoscopic analyses [3]. This discrepancy should be caused by misidentifications and negative implications on patient attention. Classification of automated disease may overcome this problem through physicians with dependable and objective diagnosis of numerous GI endoscopic images thus, reducing the diagnostic error rate, enhancing prediction, and saving medical specialists valued time [4]. As a result, Automated GI disease classification has an available field of study for achieving efficient lesion identification and classification accuracy [5].

Computer-aided diagnosis (CAD) system employs artificial intelligence (AI) and medical image processing to support radiologists in identifying diseases and analyzing the images [6]. CAD aids the radiologist in diagnosing irregularities and decision-making more quickly. Primarily, machine learning (ML) systems namely Decision Tree (DT), RF, SVM, and Naïve Bayes (NBs) are implemented for classifying the endoscopic images [7]. The effectiveness of the ML algorithm majorly depends on the detected features for developing the frameworks [8]. The main limitation of an ML method is the need a specialist experts like a gastroenterologist, to properly detect the essential features employed for classification [9], [10]. Because of the new developments in AI, Deep Learning (DL) techniques perform a crucial part in supporting radiologists in physical analysis and assisting in the identification of diseases [11]. DL algorithms can be the ability to automate feature extraction, which provides for enhancing the effectiveness of the model [12], [13]. Convolutional neural networks (CNNs) indicate superior performance for extracting features than ML techniques [14]. The prediction accuracy has been resolved by the quality and size of the database, model framework, and hyperparameter of architecture. The main challenge of the CNN approach was the need for a massive quantity of data to make a robust model [15], [16]. During the medical sector, the quantity of test and training data accessible for developing a powerful system has been restricted. In this condition, transfer learning (TL) algorithms perform a major part of designing a strong system [17].

This study presents an Endoscopic Image Analysis for Gastrointestinal Tract Disease Diagnosis using an inspired Algorithm with Deep Learning (EIAGTD-NIADL) technique. Primarily, the EIAGTD-NIADL technique uses a bilateral filtering (BF) approach. For feature extraction, the EIAGTD-NIADL technique applies an improved ShuffleNet model. To improve the efficacy of the improved ShuffleNet model, the EIAGTD-NIADL technique uses an improved spotted hyena optimizer (ISHO) algorithm. Finally, the classification process is performed by the exploitation of a stacked long short-term memory (SLSTM) method. The achieved outcome of the EIAGTD-NIADL system can be tested with benchmark medical image databases.

II. RELATED WORKS

Obayya et al. [18] presented a Modified Salp Swarm Algorithm with DL-assisted GIT Disease Classification (MSSADL-GITDC) on Endoscopic Images. This developed MSSADL-GITDC method mostly considers the analysis of wireless capsule endoscopy (WCE) images for classifying GIT. This implemented MSSADL-GITDC approach develops enhanced CapsNet architecture for extracting features but the CapsNet framework was adapted by the class attention layer (CAL). The DBN-ELM has been deployed for classifying GIT. Ramamurthy et al. [19] designed a new model for classifying endoscopy images by considering feature extraction with the help of the CNN method. This algorithm introduced was made by incorporating a current framework (for example, EfficientNet B0) with a customized CNN model termed Effimix. This implemented Effimix method utilizes an integration of excitation and squeeze layers and self-normalizing activation layers to correctly classify GI diseases. In [20], a DL algorithm was exploited for the classification of GI diseases. The pretrained process ResNetSO was fine-tuned by utilizing TL for extracting deep features from WCE images.

Su et al. [21] designed a novel and real-world technique for diagnosing GI disease from WCE images through CNN algorithms. This introduced approach applies 3 backbone networks fine-tuned and adapted by the TL method like the feature extraction, and an incorporated method exploiting ensemble learning has been trained for diagnosing GI diseases. Haile et al. [22] developed a combined NN architecture by integrating the removed features of InceptionNet and VGGNet networks to design a GI disease diagnostic framework. The DCNNs InceptionNet and VGGNet have been trained and employed for extracting features at the specified endoscopic images. Further, these removed features were combined and categorised by utilizing ML classification models namely RF, SVM, Softmax, and KNN. In [23], An innovative method was implemented dependent upon the integration of geometric features and the DCNN model. Mainly, the diseased area was extracted from specified WCE images by employing a novel method called contrast-improved colour features. Then, Geometric features have been removed from the segmented disease region. The desired features could be lastly categorized through K-NN.

Mohapatra et al. [24] introduced a smart medical technique for diagnosing numerous irregularities existing in the GI areas by implementing a CNN model and time-frequency examination. The primary stage of the analysis comprises an image preprocessing stage and then extracted predictable discrete wavelet transform (DWT) coefficients. Escobar et al. [25] recommended a method to support medical diagnostic procedures of diseases and abnormalities in the GIT dependent upon the categorization of extracted features from endoscopic images with a category of CNN and TL algorithms fine-tuning.

III. THE PROPOSED MODEL

In this study, we have derived an automated gastrointestinal tract disease detection and classification model, named the EIAGTD-NIADL system. The main objective

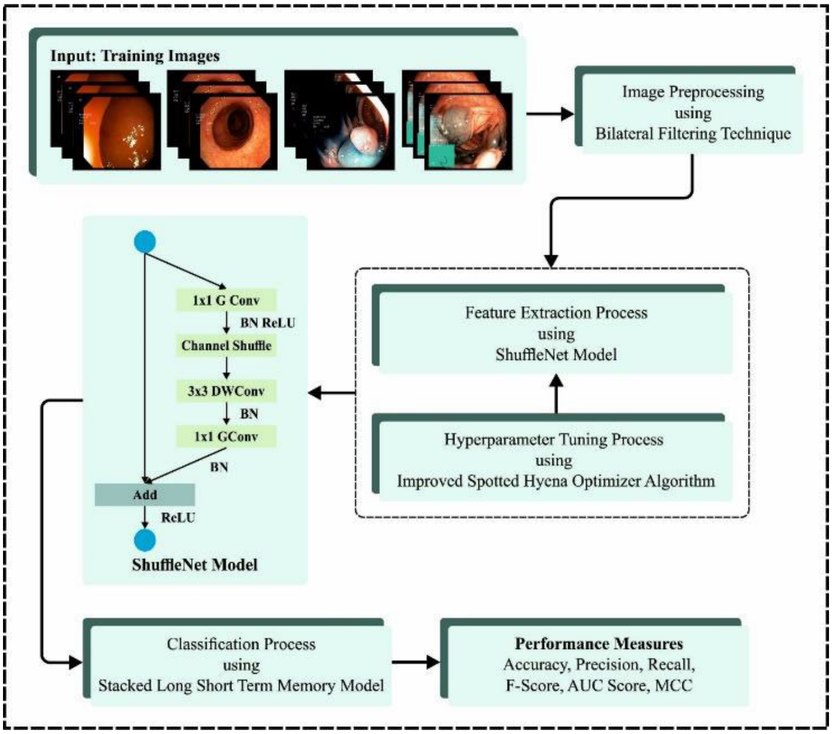

FIGURE 1. Overall process of the EIAGTD-NIADL algorithm.

of the EIAGTD-NIADL method is to test the endoscopic images using a nature-inspired method with a DL model for gastrointestinal tract disease detection and classification. The EIAGTD-NIADL technique comprises BF-based pre-processing, improved ShuffleNet feature extractor, ISHO-assisted parameter tuning, and SLSTM-based classification. Fig. 1 shows the complete process of the EIAGTD-NIADL methodology.

A. BF-BASED IMAGE PRE-PROCESSING

The BF approach is used to pre-process the input images. BF is a basic technology in medical image processing, where it acts as a robust mechanism to enhance the clarity and quality of medical imaging [26]. Whilst retaining edges and fine details by efficiently reducing artefacts and noise, BF greatly contributes to improving the accuracy of medical image analysis, aiding healthcare professionals and radiologists in making accurate diagnoses and treatment decisions. It's versatile and nature adaptive making bilateral filtering especially suitable for augmenting diagnostic images.

B. FEATURE EXTRACTION USING IMPROVED SHUFFLENET

An enhanced ShuffleNet model is applied to extract the features. The lightweight network model is a ShuffleNetV2 used to accelerate the operation and drastically decrease the size of the models without comprising the performance [27]. The breakthrough of this model is that it makes efficient use of the group convolution and channel shuffle to decrease the number of parameters and the computation amount of the models. In particular, channel shuffle is used to disrupt the channel of feature maps and recreate new feature maps to resolve the problems of worse data flow generated by the group convolutional. Too much group convolutional might result in a large MAC overhead. The output channel counts consecutively increase as the network depth upsurges, whereas the output channel counts of Conv5, Stage 2, Stage 3, and Stage 4 successively increase, the feature extraction capability is considerably improved, and the recognition performance is constantly enhanced. The fundamental architecture of ShuffleNetV2 comprises two kinds of blocks. Block1 arbitrarily splits the input channels into 2 parts: the former preserves its mapping and transfers directly downwards; the latter implements separable convolutions for extracting the image features. At the bottom of the model, the output channel of both parts is fused to double the last output channel. Next, an arbitrary mixing function can be implemented on the last resultant feature graph channel. Block 2 is used to send each feature diagram into two network branches.

In ShuffleNetV2, each feature channel has similar weights and passes through the amount of channels doubles each time Block 2. Much attention is paid to doubling the number of channels to the feature channel with a significant effect on the classification outcomes. In the meantime, the depthwise convolution applied in Block 2 has a sensitivity to the position of sensitive features, and excessive background details were maintained that easily affect the classification effects.

The attention module focuses on the research area and tries to overwhelm the role of the research area in image enhancement. In DL-CNN, the attention mechanism is split into spatial and channel attention models. Spatial attention determines the weight relationships among dissimilar pixels in the spatial domain, which enhances the weight of area pixels, allows greater consideration of the area of interest, and minimizes the weight of unwanted areas. The channel attention determines the weight relationships between the channels, which enhance the weights of key channels, and suppress the channel with slight inhibitive effects.

The SE attention module determines the weight in the channel attention model that accomplishes priority by allocating weights among dissimilar channels. It adjusts the weight based on the dissimilar feature channels, which improves the feature channel automatically with available data in the image as well as suppresses the feature channel irrelevant to the target efficiently.

C. DESIGN OF ISHO-BASED HYPERPARAMETER TUNING

In this work, the ISHO method could be implemented for the hyperparameter tuning model. The SHO relies on social activities and the relationships among hyenas [28]. It is mostly the encircling, attacking, searching, and hunting strategy of hyenas. SHO simulates the movement of spotted hyenas to accomplish a better performance. Encircling is determined by the subsequent 2 formulas.

$$\overrightarrow{\zeta_h} = \left| A.\overrightarrow{\xi_p}(x) - \overrightarrow{\xi}(x) \right| \tag{1}$$

$$\overrightarrow{\xi}(x+1) = \overrightarrow{\xi_p}(x) - B.\overrightarrow{\zeta_h} \tag{2}$$

whereas ξ_p represents the better feature vector (FV), $\xi(x)$ denotes the existing FV, and ζ_h stands for the distance to be equivalent hyena would travel to catch their target. The coefficients A and B can be measured as:

$$A = 2.d_1 \tag{3}$$

$$B = 2.h.d_2 - h \tag{4}$$

$$h = 5 - \frac{k^{th} * 5}{\max_k} \tag{5}$$

whereas, k^{th} refers to the value of existing iteration and $\max_k$ denotes the maximum round counts. The vector h has been decreased from [5-0], as represented in Eq. (5), and d_1 and d_2 define the random numbers from the interval of zero and one. The subsequent formulas map the hunting areas of spotted hyenas:

$$\overrightarrow{\zeta_h} = \left| A * \overrightarrow{\xi_h} - \overrightarrow{\xi_k} \right| \tag{6}$$

$$\overrightarrow{\xi_k} = \overrightarrow{\xi_h} - B * \overrightarrow{\zeta_h} \tag{7}$$

$$\overrightarrow{O_h} = \overrightarrow{\zeta_k} + \overrightarrow{\zeta_{k+1}} + \ldots + \overrightarrow{\zeta_{k+N}} \tag{8}$$

whereas $\overrightarrow{\xi_k}$ signifies the searching space of equivalent hyenas $\overrightarrow{O_h}$ determines the cluster of better outcomes and N represents the iteration counts that are measured as:

$$N = count_n \left(\overrightarrow{\zeta_h}, \overrightarrow{\zeta_{h+1}}, \overrightarrow{\zeta_{h+2}}, \ldots, \overrightarrow{\zeta_{h+M}} \right) \tag{9}$$

$$\overrightarrow{\zeta}(x+1) = \frac{\overrightarrow{O_h}}{N} \tag{10}$$

In which, n indicates the no. of solutions that have been in a region near optimum solution. The vector $\overrightarrow{M}$ illustrates the arbitrarily adjusted vector among 0.5 and 1. An optimum solution $\overrightarrow{\zeta}(x+1)$ supports upgrading the residual solutions at the termination of all the iterations. The search of hyenas is made sure to employ the arbitrary coefficients A and B but the exploration begins if $-1 < B < 1$ and A from zero to five; and assists as a weighted for the equivalent hyena. The optimizer method starts with the initialization of an arbitrary population, all the hyenas mark their region and with all the iterations, the coefficient h can reduced linearly. Optimum agents are then fetched after all the iterations. The ISHO algorithm can be designed by the use of Logistic Sine-Cosine Chaotic mappings.

Nowadays, chaotic mapping is commonly ma applied for generating the population initialization produced by arbitrary chaotic sequences in intelligence optimizer techniques [29]. Presently, this technique is conventional in image encryption, image processing, and other domains, and several researchers also applied it in early populations which generate intelligence optimization techniques. The most frequently utilized chaotic mappings are Logistic mapping and Sine mapping, however, the low-dimension chaotic mapping was challenging to procedure population distribution, hence The sine, Logistic dimension chaotic mapping was combined with Cosine mapping to procedure complicated chaotic mapping to address the shortcomings of worse distribution of lowest dimension mappings and it can be formulated by:

$$X_{i+1} = \cos\left(\pi \cdot (4 \cdot p \cdot X_i) \cdot (1 - X_i) + (1-p) .sin(\pi \cdot X_i) - 0.5\right) \tag{11}$$

where $p \in [0, 1]$, all the individuals in the population were considered by the rows and columns of the matrix to be the location in space. All the points in the images are assumed as individuals in the initial population, and the location and distribution of duplicate individual was observed. The mixed chaotic mapping was equally allocated, and the initialized effects of the sparrow population were more effective than the mapping effects of low-dimension chaos.

The fitness selection is an essential parameter in the ISHO method. An encoded Solution is applied to measure the goodness of the solution candidate. Then, the accuracy values are the major form exploited to generate a FF.

$$Fitness = \max(P) \tag{12}$$

$$P = \frac{TP}{TP + FP} \tag{13}$$

where FP and TP denote the false and true positive values.

D. IMAGE CLASSIFICATION USING SLSTM MODEL

Finally, the SLSTM model can be applied to image classification. LSTM approaches are deep RNN techniques that are commonly applied in several applications like time series, sentiment and language analysis, and voice detection models [30]. An RNN is a procedure of NN employed for solving sequential issues. It takes cyclic connections among several layers that support it to learn the preceding data. The output in the deep layer offers feedback as input to the other states or networks, together with the second input vectors. This recurrent connection works as a memory for the models, permitting it to learn and employ the sequence of functions as an input series. The standard RNN approach takes the drawback of being complex for training that needs to learn long-term temporal relations.

LSTM is a difficult RNN algorithm enhanced with memory units, which store data for lengthy processes. LSTM differentiates itself from a typical FFNN but it takes cycles that feed network actions in a preceding timestep as an input to the network for improving forecasts at the existing time interval. Accordingly, the recurrent connection generates a memory of previous implementations that is implicitly recorded from its hidden layer parameters. Then, it offers the optimum performances if temporal dependence from the data sequence is a vital implicit element and learning in prior steps can be needed to estimate ability trends in the future.

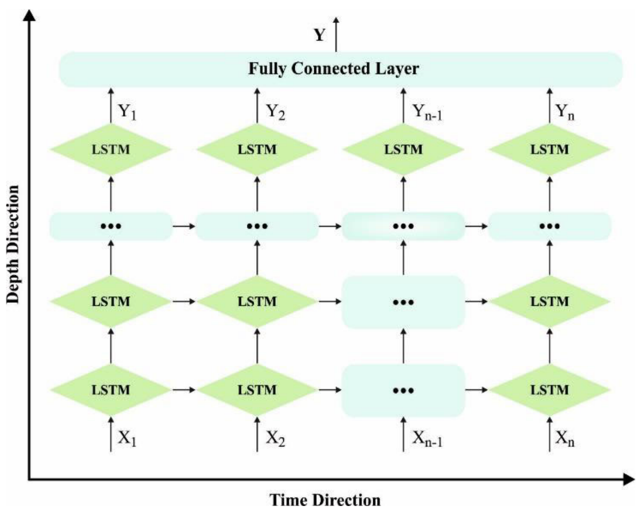

FIGURE 2. Architecture of SLSTM.

The LSTM algorithm contains 3 kinds of gates that manage the data flow such as forget, output, and input. An input gate defines that data to include in the existing input to the cell layer, the forgetting gate defines that data can be rejected in the cell layer, leaving just correct data and the resultant gate defines that data to output in the existing cell layer. The formulas for LSTM can expressed in the given below:

$$i_z = \sigma\left(W_i \cdot [h_{z-1}, x_z] + b_i\right) \tag{14}$$
$$f_z = \sigma\left(W_f \cdot [h_{z-1}, x_z] + b_f\right) \tag{15}$$
$$o_z = \sigma\left(w_o \cdot [h_{z-1}, x_z] + b_o\right) \tag{16}$$
$$\tilde{C} = tanh\left(W_C \cdot [h_{z-1}, x_z] + b_C\right) \tag{17}$$
$$C_z = f_z \odot C_{z-1} + i_z * \tilde{C}_z \tag{18}$$
$$h_z = O_z \odot tanh\,(C) \tag{19}$$

whereas h_z demonstrates the hidden layer (HL), C_z defines the cell layer, and σ implies the logistic sigmoid function to create numbers between zero and one and explains that several of all the components must be passed by the gates. $\odot$ denotes the multiplication that occurred in the data flow. Besides, *tanh* signifies the hyperbolic tangent function that ranges among $[-1, 1]$ for overcoming the gradient disappearing problems and creates a novel vector that is more to the cell layer. In a SLSTM network, multiple LSTM layers are connected sequentially, forming a deep architecture. Fig. 2 illustrates the structure of SLSTM. The output of one LSTM layer serves as the input to the next layer. Stacking LSTMs allows the network to learn difficult hierarchical representations of sequential data.

IV. RESULTS AND DISCUSSION

In this section, the performance validation of the EIAGTD-NIADL system could be analyzed using the Kvasir dataset [31], comprising 8000 samples with 8 classes as represented in Table 1. Fig. 3 depicts the sample images. The proposed model is simulated using the Python 3.8.5 tool on PC i5-8600k, GeForce 1050Ti 4GB, 16GB RAM, 250GB SSD, and 1TB HDD. The parameter settings are given as follows: learning rate: 0.01, dropout: 0.5, batch size: 5, epoch count: 50, and activation: ReLU.

TABLE 1. Details on database.

Class	Labels	No. of Instances
Dyed Lifted Polyps	C-1	1000
Dyed Resection Margins	C-2	1000
Esophagi Tis	C-3	1000
Normal-Cecum	C-4	1000
Nonnal-Pylorus	C-5	1000
Nonnal-Z-Line	C-6	1000
Polyps	C-7	1000
Ulcerative Colitis	C-8	1000
Total No. of Instances		8000

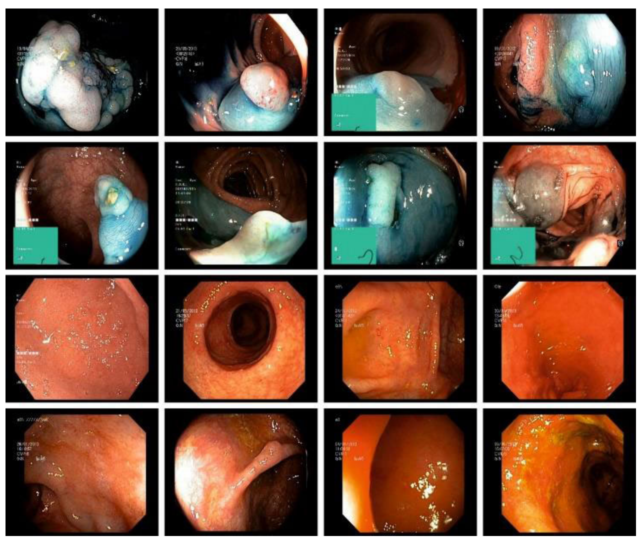

FIGURE 3. Sample endoscopic images from the Kvasir dataset.

IEEE Access

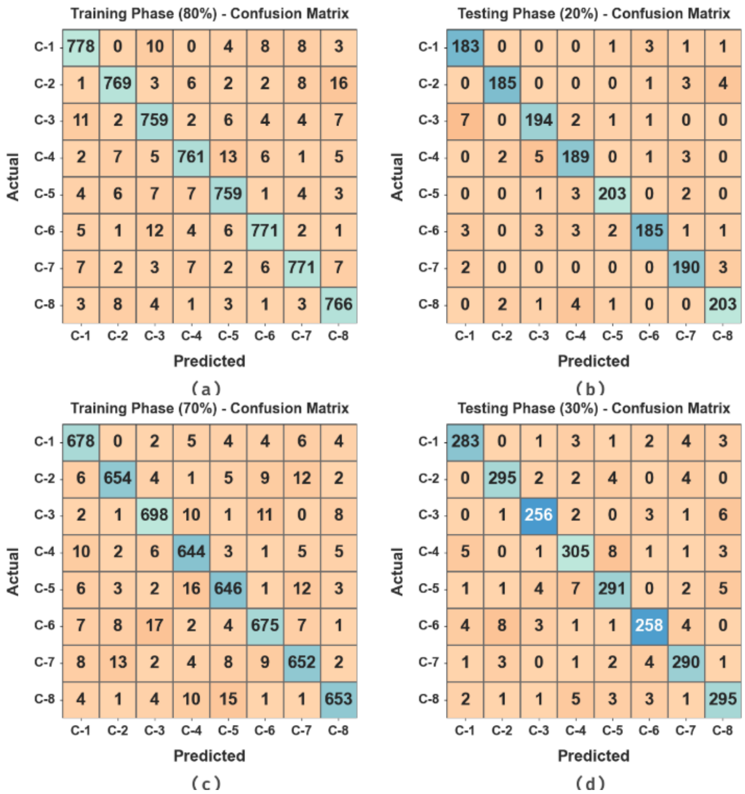

FIGURE 4. (a-b) Confusion matrices for 80:20 of TR phase/TS phase and (c-d) 70:30 of TR phase/TS phase.

TABLE 2. Disease detection analysis of EIAGTD-NIADL model with 80:20 of TR phase/TS phase.

Class	$Accu_y$	$Prec_n$	$Reca_l$	F_{Score}	AUC	MCC
TR Phase (80%)						
C-1	98.97	95.93	95.93	95.93	97.67	95.34
C-2	99.00	96.73	95.29	96.00	97.41	95.44
C-3	98.75	94.52	95.47	94.99	97.34	94.28
C-4	98.97	96.57	95.13	95.84	97.32	95.26
C-5	98.94	95.47	95.95	95.71	97.66	95.11
C-6	99.08	96.50	96.13	96.31	97.82	95.79
C-7	99.00	96.25	95.78	96.01	97.62	95.44
C-8	98.98	94.80	97.08	95.93	98.17	95.36
Avg.	98.96	95.85	95.85	95.84	97.63	95.25
TS Phase (20%)						
C-1	98.88	93.85	96.83	95.31	97.99	94.69
C-2	99.25	97.88	95.85	96.86	97.79	96.44
C-3	98.69	95.10	94.63	94.87	96.96	94.11
C-4	98.56	94.03	94.50	94.26	96.82	93.44
C-5	99.31	97.60	97.13	97.36	98.38	96.97
C-6	98.81	96.86	93.43	95.12	96.50	94.46
C-7	99.06	95.00	97.44	96.20	98.36	95.68
C-8	98.94	95.75	96.21	95.98	97.78	95.37
Avg.	98.94	95.76	95.75	95.75	97.57	95.14

The confusion matrices achieved by the EIAGTD-NIADL approach with 80:20 and 70:30 of the TR phase/TS phase are given in Fig. 4. The outcomes signified the efficient identification and classification of all 8 classes.

The disease detection results of the EIAGTD-NIADL technique on 80:20 of the TR phase/TS phase are presented in Table 2 and Fig. 5.

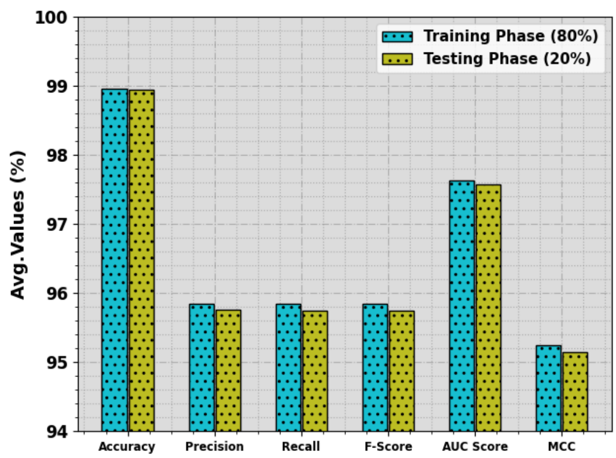

FIGURE 5. Average of EIAGTD-NIADL system at 80:20 of TR phase/TS phase.

In Table 3 and Fig. 6, the disease detection outcome of the EIAGTD-NIADL system at 70:30 of the TR phase/TS phase is depicted. The achieved values depicted the better performance of the EIAGTD-NIADL algorithm on all classes. With 70% TR phase, the EIAGTD-NIADL technique attains average $accu_y$, $prec_n$, $reca_l$, F_{score}, AUC_{score}, and MCC of 98.66%, 94.65%, 96.64%, 94.64%, 96.94%, and 93.88% correspondingly. Next, with a 30% TS phase, the EIAGTD-NIADL methodology achieves average $accu_y$, $prec_n$, $reca_l$, F_{score}, AUC_{score}, and MCC of 98.68%, 97.74%, 94.70%, 94.72%, 96.97%, and 93.96% correspondingly.

TABLE 3. Disease detection outcome of EIAGTD-NIADL algorithm at 70:30 of TR phase/TS phase.

Class Labels	$Accu_y$	$Prec_n$	$Reca_l$	F_{Score}	AUC_{Score}	MCC
TR Phase (70%)						
C-1	98.79	94.04	96.44	95.22	97.78	94.54
C-2	98.80	95.89	94.37	95.13	96.90	94.45
C-3	98.75	94.97	95.49	95.23	97.36	94.51
C-4	98.57	93.06	95.27	94.15	97.15	93.35
C-5	98.52	94.17	93.76	93.96	96.47	93.12
C-6	98.54	94.94	93.62	94.27	96.44	93.44
C-7	98.41	93.81	93.41	93.61	96.27	92.70
C-8	98.91	96.31	94.78	95.54	97.13	94.92
Average	98.66	94.65	94.64	94.64	96.94	93.88
TS Phase (30%)						
C-1	98.88	95.61	95.29	95.45	97.33	94.81
C-2	98.92	95.47	96.09	95.78	97.71	95.16
C-3	98.96	95.52	95.17	95.34	97.30	94.76
C-4	98.33	93.56	94.14	93.85	96.56	92.88
C-5	98.38	93.87	93.57	93.72	96.33	92.79
C-6	98.58	95.20	92.47	93.82	95.93	93.03
C-7	98.79	94.46	96.03	95.24	97.61	94.55
C-8	98.58	94.25	94.86	94.55	97.00	93.74
Average	98.68	94.74	94.70	94.72	96.97	93.96

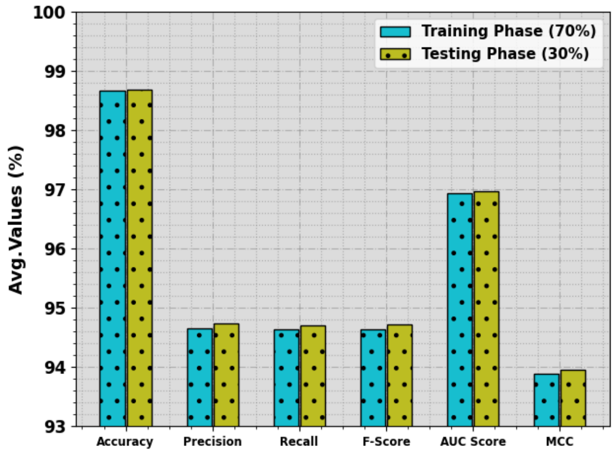

FIGURE 6. Average of EIAGTD-NIADL model at 70:30 of TR phase/TS phase.

The training and validation accuracy curves of the EIAGTD-NIADL approach at 80:20 of the TR phase/TS phase depicted in Fig. 7, offer valuable insights into the outcome of the EIAGTD-NIADL approach over several epochs. These curves highlight the essential insights into the learning process and the model's ability to generalize. Besides, it can be noticeable that there is a consistency improvement in the TR and TS accuracy over maximum epochs. It detected the model's capacity to learn and recognize patterns within both the training and testing databases. The increasing testing accuracy proposes that the model not only adjusts to the training data but also excels in making accurate predictions on previously unseen data, highlighting its robust generalization capabilities.

FIGURE 7. $Accu_y$ curve of EIAGTD-NIADL algorithm at 80:20 of TR phase/TS phase.

In Fig. 6, we signify a comprehensive view of the TR and TS loss outcomes for the EIAGTD-NIADL approach at 80:20 of the TR phase/TS phase across various epochs. The TR loss progressively reduces as the model improves its weights to diminish classification errors on both the TR and TS databases. These loss curves offer a clear picture of how well the model aligns with the training data, underlining its capability to efficiently hold patterns in both datasets. It is worth noting that the proposed model incessantly refines its parameters to reduce the discrepancies between the predictive and the actual TR classes.

With respect to the precision-recall curve as provided in Fig. 9, the outcomes clearly confirm that the EIAGTD-NIADL model at 80:20 of TR phase/TS phase steadily accomplishes improved precision-recall values across every class. The outcomes highlight the effectual capability of the model in the discrimination of different classes, highlighting the effectiveness in the detection of classes.

Moreover, in Fig. 10, we present ROC curves produced by the EIAGTD-NIADL approach at 80:20 of the TR phase/TS phase, which excels in differentiating among the classes. These curves offer valuable insights into the balance among TPR and FPR across different classification thresholds and epochs. The outcomes highlight the accurate classification

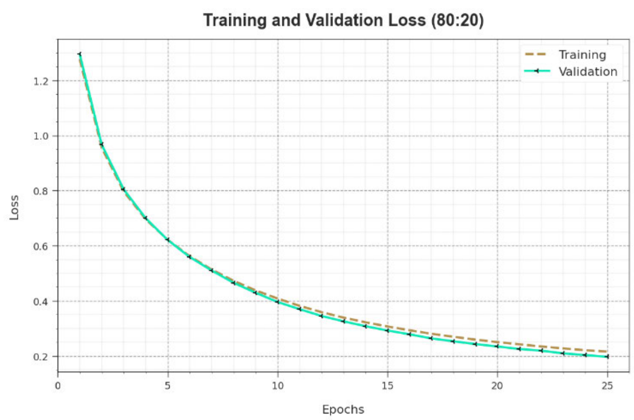

FIGURE 8. Loss curve of EIAGTD-NIADL algorithm with 80:20 of TR phase/TS phase.

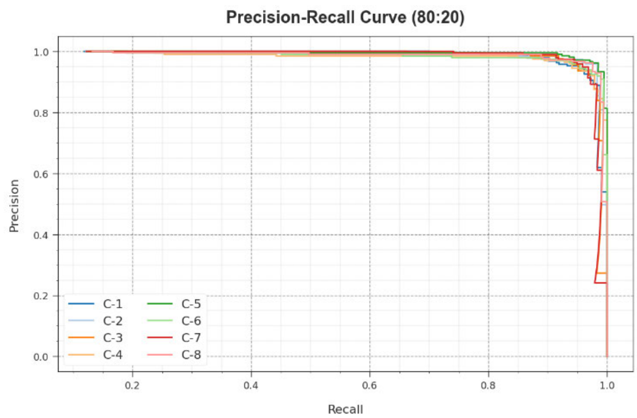

FIGURE 9. PR curve of EIAGTD-NIADL algorithm with 80:20 of TR phase/TS phase.

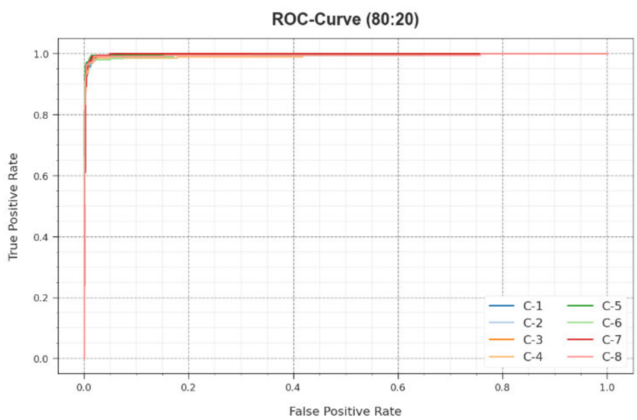

FIGURE 10. ROC curve of EIAGTD-NIADL algorithm at 80:20 of TR phase/TS phase.

outcome under distinct classes, highlighting the performance in tackling various classification challenges.

To investigate the improved effectiveness of the EIAGTD-NIADL technique, a brief comparative analysis is examined in Table 4 and Fig. 11 [18], [32]. The results pointed out that the EIAGTD-NIADL methodology reaches better performance. Based on $prec_n$, the EIAGTD-NIADL technique offers increasing $prec_n$ of 95.85% while the MSSADL-GITDC, ECA-Net Model, DL-OCT, LSMT-CNN, Attention-Guided CNN, VGG16, and LR Tree models obtain decreasing $prec_n$ values of 92.16%, 89%, 90.09%, 90.14%, 91.44%, 92.01%, and 87.04% respectively.

Meanwhile, based on $reca_l$, the EIAGTD-NIADL method attains an enhanced $reca_l$ of 95.85% while the MSSADL-GITDC, ECA-Net Model, DL-OCT, LSMT-CNN, Attention-Guided CNN, VGG16, and LR Tree approach gains lesser $reca_l$ values of 92.13%, 91.24%, 90.29%, 91.75%, 90.32%, 90.13%, and 89.17% correspondingly. At last, based on $accu_y$, the EIAGTD-NIADL methodology achieves a maximal $accu_y$ of 98.96% while the MSSADL-GITDC, ECA-Net Model, DL-OCT, LSMT-CNN, Attention-Guided CNN, VGG16, and LR Tree systems achieve lesser $accu_y$ values of 98.03%, 92.68%, 90.20%, 92.82%, 93.25%, 96.02%, and 94.13% correspondingly.

TABLE 4. Comparative outcome of EIAGTD-NIADL algorithm with recent approaches [18], [32].

Methods	$Prec_n$	$Reca_l$	$Accu_y$	F_{score}
EIAGTD-NIADL	95.85	95.85	98.96	95.84
MSSADL-GITDC	92.16	92.13	98.03	92.11
ECA-Net Model	89.00	91.24	92.68	88.42
DL-OCT Model	90.09	90.29	90.20	89.00
LSMT-CNN	90.14	91.75	92.82	91.98
Attention-Guided CNN	91.44	90.32	93.25	91.05
VGG16 Model	92.01	90.13	96.02	91.24
LR Tree Algorithm	87.04	89.17	94.13	91.53

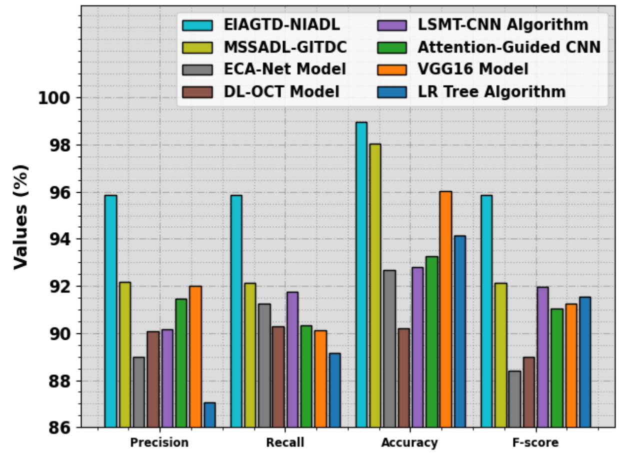

FIGURE 11. Comparative outcome of EIAGTD-NIADL algorithm with recent approaches.

These results confirmed the supremacy of the EIAGTD-NIADL technique.

V. CONCLUSION

In this study, we have derived an automated gastrointestinal tract disease detection and classification model, named EIAGTD-NIADL technique. The main objective of the EIAGTD-NIADL system is to examine the endoscopic images using a nature-inspired method with a DL model for gastrointestinal tract disease detection and classification. The EIAGTD-NIADL technique comprises BF-based pre-processing, improved ShuffleNet feature extractor, ISHO-assisted parameter tuning, and SLSTM-based classification. The achieved outcomes of the EIAGTD-NIADL method are examined on the benchmark Kvasir dataset. The obtained results demonstrate the promising results of the EIAGTD-NIADL algorithm over other models with a maximum accuracy of 98.96%. The improved ability of the EIAGTD-NIADL approach is utilized for accurately analyzing endoscopic images and videos leading to better diagnostic accuracy. This has great to decrease misdiagnoses and ensure that patients receive the correct treatment promptly. By providing more correct disease classification and monitoring, the EIAGTD-NIADL supports the progress of personalized treatment plans for patients. In summary, the EIAGTD-NIADL approach has practical implications that comprise better diagnostic accuracy, early recognition, real-time medical support, personalized treatment, cost savings, better patient outcomes, and contributions to medical training and research.

Future work is to observe the computational complexity of the presented method on real-time databases. For future work, the EIAGTD-NIADL technique can be extended to contain a broader spectrum of gastrointestinal diseases, actually improving its clinical applicability. Furthermore, the integration of real-time endoscopic image analysis and more refinement of optimizer approaches offer avenues for enhancing the model's responsiveness and diagnostic accuracy, ultimately helping patient care and medical decision-making.

ACKNOWLEDGMENT

The authors extend their appreciation to the Deanship of Scientific Research at King Khalid University for funding this work through large group Research Project under grant number (RGP2/29/44). Princess Nourah bint Abdulrahman University Researchers Supporting Project number (PNURSP2023R161), Princess Nourah bint Abdulrahman University, Riyadh, Saudi Arabia. Research Supporting Project number (RSP2022R444), King Saud University, Riyadh, Saudi Arabia. This study is partially funded by the Future University in Egypt (FUE).

REFERENCES

[1] P. Bhardwaj, S. Kumar, and Y. Kumar, "A comprehensive analysis of deep learning-based approaches for the prediction of gastrointestinal diseases using multi-class endoscopy images," *Arch. Comput. Methods Eng.*, vol. 30, no. 7, pp. 4499–4516, Sep. 2023.

[2] I. M. Dheir and S. S. Abu-Naser, "Classification of anomalies in the gastrointestinal tract using deep learning," Tech. Rep., 2022.

[3] E. Sivari, E. Bostanci, M. S. Guzel, K. Acici, T. Asuroglu, and T. E. Ayyildiz, "A new approach for gastrointestinal tract findings detection and classification: Deep learning-based hybrid stacking ensemble models," *Diagnostics*, vol. 13, no. 4, p. 720, Feb. 2023.

[4] J. Escobar, K. Sanchez, C. Hinojosa, H. Arguello, and S. Castillo, "Accurate deep learning-based gastrointestinal disease classification via transfer learning strategy," in *Proc. 23rd Symp. Image, Signal Process. Artif. Vis. (STSIVA)*, Sep. 2021, pp. 1–5.

[5] I. Iqbal, K. Walayat, M. U. Kakar, and J. Ma, "Automated identification of human gastrointestinal tract abnormalities based on deep convolutional neural network with endoscopic images," *Intell. Syst. with Appl.*, vol. 16, Nov. 2022, Art. no. 200149.

[6] D. Jha, S. Ali, S. Hicks, V. Thambawita, H. Borgli, P. H. Smedsrud, T. de Lange, K. Pogorelov, X. Wang, P. Harzig, and M. T. Tran, "A comprehensive analysis of classification methods in gastrointestinal endoscopy imaging," *Med. Image Anal.*, vol. 70, May 2021, Art. no. 102007.

[7] Ş. Öztürk and U. Özkaya, "Residual LSTM layered CNN for classification of gastrointestinal tract diseases," *J. Biomed. Informat.*, vol. 113, Jan. 2021, Art. no. 103638.

[8] C. Gamage, I. Wijesinghe, C. Chitraranjan, and I. Perera, "GI-Net: Anomalies classification in gastrointestinal tract through endoscopic imagery with deep learning," in *Proc. Moratuwa Eng. Res. Conf. (MERCon)*, Jul. 2019, pp. 66–71.

[9] H. Li, X. Hou, R. Lin, M. Fan, S. Pang, L. Jiang, Q. Liu, and L. Fu, "Advanced endoscopic methods in gastrointestinal diseases: A systematic review," *Quant. Imag. Med. Surgery*, vol. 9, no. 5, pp. 905–920, May 2019.

[10] H. Chen and J. J. Y. Sung, "Potentials of AI in medical image analysis in gastroenterology and hepatology," *J. Gastroenterol. Hepatol.*, vol. 36, no. 1, pp. 31–38, Jan. 2021.

[11] H. Ali, M. Sharif, M. Yasmin, M. H. Rehmani, and F. Riaz, "A survey of feature extraction and fusion of deep learning for detection of abnormalities in video endoscopy of gastrointestinal-tract," *Artif. Intell. Rev.*, vol. 53, no. 4, pp. 2635–2707, Apr. 2020.

[12] S. Ali, "Deep learning for detection and segmentation of artefact and disease instances in gastrointestinal endoscopy," *Med. Image Anal.*, vol. 70, May 2021, Art. no. 102002.

[13] M. N. Noor, M. Nazir, S. A. Khan, I. Ashraf, and O.-Y. Song, "Localization and classification of gastrointestinal tract disorders using explainable AI from endoscopic images," *Appl. Sci.*, vol. 13, no. 15, p. 9031, Aug. 2023.

[14] S. M. Fati, E. M. Senan, and A. T. Azar, "Hybrid and deep learning approach for early diagnosis of lower gastrointestinal diseases," *Sensors*, vol. 22, no. 11, p. 4079, May 2022.

[15] V. Raut, R. Gunjan, V. V. Shete, and U. D. Eknath, "Gastrointestinal tract disease segmentation and classification in wireless capsule endoscopy using intelligent deep learning model," *Comput. Methods Biomech. Biomed. Eng., Imag. Visualizat.*, vol. 11, no. 3, pp. 606–622, May 2023.

[16] M. A. Khan, N. Sahar, W. Z. Khan, M. Alhaisoni, U. Tariq, M. H. Zayyan, Y. J. Kim, and B. Chang, "GestroNet: A framework of saliency estimation and optimal deep learning features based gastrointestinal diseases detection and classification," *Diagnostics*, vol. 12, no. 11, p. 2718, Nov. 2022.

[17] J. Yogapriya, V. Chandran, M. G. Sumithra, P. Anitha, P. Jenopaul, and C. S. G. Dhas, "Gastrointestinal tract disease classification from wireless endoscopy images using pretrained deep learning model," *Comput. Math. Methods Med.*, vol. 2021, pp. 1–12, Sep. 2021.

[18] M. Obayya, F. N. Al-Wesabi, M. Maashi, A. Mohamed, M. A. Hamza, S. Drar, I. Yaseen, and M. I. Alsaid, "Modified salp swarm algorithm with deep learning based gastrointestinal tract disease classification on endoscopic images," *IEEE Access*, vol. 11, pp. 25959–25967, 2023.

[19] K. Ramamurthy, T. T. George, Y. Shah, and P. Sasidhar, "A novel multi-feature fusion method for classification of gastrointestinal diseases using endoscopy images," *Diagnostics*, vol. 12, no. 10, p. 2316, Sep. 2022.

[20] Y. Oukdach, Z. Kerkaou, M. El Ansari, L. Koutti, and A. F. El Ouafdi, "Gastrointestinal diseases classification based on deep learning and transfer learning mechanism," in *Proc. 9th Int. Conf. Wireless Netw. Mobile Commun. (WINCOM)*, Oct. 2022, pp. 1–6.

[21] Q. Su, F. Wang, D. Chen, G. Chen, C. Li, and L. Wei, "Deep convolutional neural networks with ensemble learning and transfer learning for automated detection of gastrointestinal diseases," *Comput. Biol. Med.*, vol. 150, Nov. 2022, Art. no. 106054.

[22] M. B. Haile, A. O. Salau, B. Enyew, and A. J. Belay, "Detection and classification of gastrointestinal disease using convolutional neural network and SVM," *Cogent Eng.*, vol. 9, no. 1, Dec. 2022, Art. no. 2084878.

[23] M. Sharif, M. Attique Khan, M. Rashid, M. Yasmin, F. Afza, and U. J. Tanik, "Deep CNN and geometric features-based gastrointestinal tract diseases detection and classification from wireless capsule endoscopy images," *J. Experim. Theor. Artif. Intell.*, vol. 33, no. 4, pp. 577–599, Jul. 2021.

[24] S. Mohapatra, J. Nayak, M. Mishra, G. K. Pati, B. Naik, and T. Swarnkar, "Wavelet transform and deep convolutional neural network-based smart healthcare system for gastrointestinal disease detection," *Interdiscipl. Sci., Comput. Life Sci.*, vol. 13, no. 2, pp. 212–228, Jun. 2021.

[25] J. P. Escobar, N. Gomez, K. Sanchez, and H. Arguello, "Transfer learning with convolutional neural network for gastrointestinal diseases detection using endoscopic images," in *Proc. IEEE Colombian Conf. Appl. Comput. Intell. (IEEE ColCACI)*, Colombia, Aug. 2020, pp. 1–6.

[26] V. Sathiyamoorthi, A. K. Ilavarasi, K. Murugeswari, S. T. Ahmed, B. A. Devi, and M. Kalipindi, "A deep convolutional neural network based computer aided diagnosis system for the prediction of Alzheimer's disease in MRI images," *Measurement*, vol. 171, Feb. 2021, Art. no. 108838.

[27] X. Xu, Y. Zhang, H. Cao, D. Yang, L. Zhou, and H. Yu, "Recognition of edible fungi fruit body diseases based on improved ShuffleNetV2," *Agronomy*, vol. 13, no. 6, p. 1530, May 2023.

[28] H. Mohyuddin, S. K. R. Moosavi, M. H. Zafar, and F. Sanfilippo, "A comprehensive framework for hand gesture recognition using hybrid-metaheuristic algorithms and deep learning models," *Array*, vol. 19, Sep. 2023, Art. no. 100317.

[29] C. Yang, H. Yang, D. Zhu, Y. Hu, Y. Zhang, H. Ma, and Z. Huang, "Chaotic sparrow search algorithm with manta ray spiral foraging for engineering optimization," *Syst. Sci. Control Eng.*, vol. 11, no. 1, Dec. 2023, Art. no. 2249021.

[30] S. H. Almuhaini and N. Sultana, "Bayesian-optimization-based long short-term memory (LSTM) super learner approach for modeling long-term electricity consumption," *Sustainability*, vol. 15, no. 18, p. 13409, Sep. 2023.

[31] *Kvasir*. Accessed: Jun. 12, 2023. [Online]. Available: https://datasets.simula.no/kvasir/

[32] Z. M. Lonseko, P. E. Adjei, W. Du, C. Luo, D. Hu, L. Zhu, T. Gan, and N. Rao, "Gastrointestinal disease classification in endoscopic images using attention-guided convolutional neural networks," *Appl. Sci.*, vol. 11, no. 23, p. 11136, Nov. 2021.